PAPER

Capacity and Reliability of Ionosphere Communication Channel Based on Multi-Carrier Modulation Technique and LUF-MUF Variation

Varuliantor DEAR[†,††a)], **Annis SIRADJ MARDIANI**[††], **Nandang DEDI**[††], **Prayitno ABADI**[†††,††††], ***Nonmembers***, **Baud HARYO PRANANTO**[†], ***Member***, ***and*** **ISKANDAR**[†], ***Nonmember***

SUMMARY Low capacity and reliability are the challenges in the development of ionosphere communication channel systems. To overcome this problem, one promising and state-of-the-art method is applying a multi-carrier modulation technique. Currently, the use of multi-carrier modulation technique is using a single transmission frequency with a bandwidth is no more than 24 kHz in real-world implementation. However, based on the range of the minimum and maximum ionospheric plasma frequency values, which could be in the MHz range, the use of these values as the main bandwidth in multi-carrier modulation techniques can optimize the use of available channel capacity. In this paper, we propose a multi-carrier modulation technique in combination with a model variation of Lowest Usable Frequency (LUF) and Maximum Usable Frequency (MUF) values as the main bandwidth to optimize the use of available channel capacity while also maintaining its reliability by following the variation of the ionosphere plasma frequency. To analyze its capacity and reliability, we performed a numeric simulation using a LUF-MUF model based on Long Short Term-Memory (LSTM) and Advanced Stand Alone Prediction System (ASAPS) in Near Vertical Incidence Skywave (NVIS) propagation mode with the assumption of perfect synchronization between transmitter and receiver with no Doppler and no time offsets. The results show the achievement of the ergodic channel capacity varies for every hour of the day, with values in the range of 10 Mbps and 100 Mbps with 0 to 20 dB SNR. Meanwhile, the reliability of the system is in the range of 8% to 100% for every hour of one day based on two different Mode Reliability calculation scenarios. The results also show that channel capacity and system reliability optimization are determined by the accuracy of the LUF-MUF model.

key words: *ionosphere communication channel, capacity, reliability, multi-carrier, LUF, MUF*

1. Introduction

The main challenge of the ionospheric communication channel system is its low channel capacity and reliability. The low channel capacity is due to the multipath fading environment and the coherent bandwidth limitations [1], [2]. While the low-reliability main factor is caused by the boundary of the transmission frequency value, which follows the variation of the ionosphere plasma frequency [3]. To overcome the low capacity issue, a multi-carrier modulation technique such as Orthogonal Frequency Division Multiplexing (OFDM) is used as one of the solutions, with the purpose to avoid frequency selective fading [4]–[8]. To overcome the low reliability issue, a management frequency approach [9]–[11], along with the implementation of adaptive selection frequencies such as the Automatic Link Establishment (ALE) technique, employed in the system [12]–[14]. This technique enables the system to follow the variations in ionospheric plasma frequencies in order to guarantee the success of radio wave propagation from transmitter to receiver. Those approaches are known as the state-of-the-art methods in the development of the ionospheric communication channel system.

Currently, the use of a multi-carrier modulation technique in the ionosphere communication channel system uses a conventional main bandwidth which values are 3 kHz (narrowband HF) [15]–[19] and 24 kHz (wideband HF) [4], [20]–[22]. Meanwhile, the adaptive technique uses an analysis of data link quality from the sounding process to select a single frequency with a narrow bandwidth [23], [24]. Those combined approaches improve the reliability of the system by following the ionosphere plasma variation and increasing the channel capacity up to 9.6 kbps in the real-world implementation [25]. However, based on the range of minimum and maximum ionosphere frequency plasma values, which are in the range of MHz [3], [10], [26], the utilization of this frequency range as the main bandwidth of a multi-carrier modulation technique is quite promising. The utilization of the ionosphere frequency plasma range as the main bandwidth of the multi-carrier modulation technique could potentially optimize the use of available channel capacity while also maintaining its reliability. In this paper, we propose the multi-carrier modulation technique with a combination of the Lowest Usable Frequency (LUF) - Maximum Usable Frequency (MUF) variations in the ionosphere communication channel system and examine its capacity and reliability. The proposed system uses the variations of the LUF-MUF value from a model and uses it as the main bandwidth, where its maximum value could be more than

Manuscript received July 27, 2023.
Manuscript revised September 26, 2023.
Manuscript publicized January 30, 2024.

[†]The authors are with School of Electrical Engineering and Informatics, Institute Technology Bandung, Jl. Ganesha 20 West Java, Indonesia.
[††]The authors are with Space Research Center, National Research and Innovation Agency, Jl. Sangkuriang, Dago Bandung, Indonesia.
[†††]The author is with Research Center for Climate and Atmosphere, National Research and Innovation Agency, Jl. Sangkuriang Bandung, Indonesia.
[††††]The author is with School of Electrical Engineering, Telkom University, Kab. Bandung, Indonesia.
a) E-mail: varuliantor.dear@brin.go.id
DOI: 10.23919/transcom.2023EBP3122

10 MHz. For the sub-carrier bandwidth, the bandwidth coherent value based on the International Telecommunication Union's (ITU) recommendation is used, where its value is in the range of kHz [27]. To analyze its capacity and reliability, we performed a numeric simulation using a LUF-MUF model based on Long Short-Term Memory (LSTM) and Advanced Stand Alone Prediction System (ASAPS) for Near Vertical Incidence Skywave (NVIS) propagation mode. To get a comprehensive explanation, the structure of this paper is presented as follows: In Sect. 2 we discuss the variation of the ionosphere and its channel capacity and reliability calculation. In Sect. 3, we explain the main concept of the multi-carrier modulation technique with a combination of LUF-MUF variation and its capacity and reliability analysis method. In Sect. 4, we show and discuss the numerical simulation result. In the last section, we conclude this paper.

2. Theoretical Background

2.1 Variation of Ionosphere Channel

As a radio wave propagation medium in the High Frequency (HF) radio spectrum, the earth's ionosphere is formed by the electrons which resulted from atmosphere ionization at 60 to 2000 km altitudes. The formation of the ionosphere layers is determined by the space weather dynamics with the main source is solar activity radiation [28]. The dynamic formation of the ionosphere layer causes the frequency of radio waves that can propagate in the ionosphere layer to vary in time and place [3]. Variations of the radio wave frequency values that can be reflected by the ionosphere layer could refer to the critical frequency value of the ionospheric F layer (f_oF2) which has daily, seasonal, and solar cycle activity variations [28]. For application in ionospheric channel communication, the f_oF2 value can be converted into the lower limit and upper limit of reflected frequency, namely the Lowest Usable Frequency (LUF) and Maximum Usable Frequency (MUF). Therefore, to guarantee the propagation of radio waves from transmitter to receiver, the transmission frequency values should be selected between the LUF and MUF values.

The calculation of LUF and MUF is based on the geometry of the transmitter and receiver locations and is expressed by the equation as follows:

$$MUF = \alpha . f_oF2 \tag{1}$$

and

$$LUF = \alpha . f_{min} \tag{2}$$

with α is the geometry factors of transmitter and receiver locations which could be expressed using equations:

$$\alpha = \frac{\sqrt{h^2 + d^2}}{h} \tag{3}$$

h is the height of the ionosphere layers, and d is the distance between the transmitter and receiver. For Near Vertical Incidence Skywave (NVIS) propagation mode, where the distance of transmitter and receiver is less than 300 km, the value of α is equal to 1. The values of LUF and MUF directly follow the f_{min} and f_oF2 values [29], [30].

2.2 Channel Capacity

Besides being known as a channel that has temporal and spatial variations, the ionosphere's physical properties also cause radio wave propagation from the transmitter to the receiver to experience more than one path, known as a multipath channel. As a multipath fading channel, ionospheric channel capacity can be calculated by the following equation:

$$C = \int_{-\infty}^{\infty} B \log_2(1 + \gamma) p(\gamma) d\gamma \tag{4}$$

where C is the capacity in units of bits per second (bps). B is the coherent bandwidth (Hz), γ is the signal to noise ratio (SNR) value, and $p(\gamma)$ is the probability density function (pdf) of the SNR value, which follows the variation of the channel realization gain value. The channel capacity in the above equation is called the ergodic capacity, as it is known as a random process. For the upper limit of the channel capacity, the calculation using the Additive White Gaussian Noise (AWGN) channel could be used, which is expressed in the equation as follows:

$$C = B \log_2(1 + \overline{\gamma}) \tag{5}$$

with $\overline{\gamma}$ is the average of SNR. For the calculation of the total channel capacity using a multi-carrier modulation technique where each sub-channel is independent and identically distributed (i.i.d), the total ergodic capacity of the system could be expressed as follows:

$$C_{tot} = \Sigma_{k=1}^{K} B \log_2(1 + \gamma_k) p(\gamma_k) \tag{6}$$

with

$$\gamma_k = \frac{|g_k|^2 P_k}{N_k B_k} \tag{7}$$

g is the realization of the channel gain for each of the k sub-carriers, P is the transmitted power, N is the noise spectral density, and B is the sub-carrier bandwidth with its values below the coherent bandwidth of the channel.

In addition to ergodic capacity, the calculation of multipath fading channel capacity can be expressed by outage capacity. Outage capacity is the probability of transmission failure based on specified criteria, such as minimum SNR. Outage capacity is expressed using the equation as follows:

$$C_{outage} = P_r(\log_2(1 + \gamma) < r) \tag{8}$$

where $Pr(.)$ is the probability function and r is the minimum data rate threshold with an acceptable error value. Outage capacity also has meaning as a measure of system reliability.

2.3 Reliability of Ionosphere Communication System

To calculate the reliability of the ionospheric channel communication system, there are six types of reliability levels

stated by the International Telecommunication Union (ITU) [31], namely: Mode Reliability, Circuit Reliability, Reception Reliability, Path Reliability, Communication Reliability, and Service Reliability. Mode Reliability (MR) is the basic level of ionospheric communication system reliability according to the limitations of the transmission frequency that could propagate in the skywave mode. In simple terms, the non-zero value of the Mode Reliability level is determined by the selection of the transmission frequency value in the range of LUF - MUF values. The Circuit Reliability is a calculation of communication circuit reliability based on the performance of a selected transmission frequency, such as the minimum SNR value limit. The Circuit Reliability calculation also includes the Mode Reliability calculation and is used as a basis for calculating the reliability level of a communication circuit, which is known as the Basic Circuit Reliability (BCR). For digital modulation, the BCR calculation is expressed by the equation as follows:

$$BCR(\%) = R_{SN}.R_T.R_F \tag{9}$$

where R_{SN} is the probability of achieving the SNR minimum (SN_o). R_T s the probability that the required time spread at a level of -10 dB relative to the peak signal amplitude is not exceeded. R_F is the probability that the required frequency dispersion at a level of -10 dB relative to the peak signal amplitude is not exceeded. To calculate R_{SN}, there are two equations that could be selected based on the condition, which are:

$$\begin{aligned} R_{SN} &= 130 - 80/[1 + (SN_m - SN_o)/D_l] \quad \text{for } SN_m \geq SN_o \\ &= 80/[1 + (SN_o - SN_m)/D_u] - 30 \quad \text{for } SN_m < SN_o \end{aligned} \tag{10}$$

with SN_m is the monthly median SNR value. D_u and D_l are the upper decile and lower decile deviation of monthly median SNR values, respectively. For calculating R_T, there are equations that are also based on two different conditions, which are:

$$\begin{aligned} R_T &= 130 - 80/[1 + (T_o - T_m)/D_{Tu}] \quad \text{for } T_m \leq T_o \\ &= 80/[1 + (T_m - T_o)/D_{Tl}] - 30 \quad \text{for } T_m > T_o \end{aligned} \tag{11}$$

with T_m is the monthly median time spread, D_{Tu} and D_{Tl} are the lower decile and upper decile deviation of monthly median time spread values, respectively. For calculating R_F, the equations based on two conditions that could be used are:

$$\begin{aligned} R_F &= 130 - 80/[1 + (F_o - F_m)/D_{Fu}] \quad \text{for } F_m \leq F_o \\ &= 80/[1 + (F_m - F_o)/D_{Fl}] - 30 \quad \text{for } F_m > F_o \end{aligned} \tag{12}$$

where F_m is the monthly median frequency dispersion,D_{Fu} and D_{Fl} are the upper decile and lower decile deviation of monthly median frequency dispersion values, respectively.

The SN_m, R_T, and R_F values could be obtained from ionospheric physical models such as VOACAP [32]. While the upper and lower decile values for those parameters could be selected from the ITU document [31]. To determine the SNo value, the BER curve as a function of SNR could be used based on the accepted minimum BER value.

For communication circuits that use more than one transmission frequency, the calculation of reliability is done using Basic Reception Reliability (BRR) which is expressed by the equation as follows:

$$BRR(\%) = 100[1 - \prod_{k=1}^{K}(1 - \frac{BCR(f_k)}{100})] \tag{13}$$

with $BCR(f_k)$ is the basic circuit reliability of each carrier frequency.

3. Multi-Carrier Modulation with LUF-MUF Variation

The basic form of multi-carrier modulation is dividing the data stream into multiple sub-streams that are transmitted over different orthogonal subchannels centered at different sub-carrier frequencies [33]. In this study, the proposed block diagram of the multi-carrier modulation technique with a combination of LUF-MUF variations in the ionosphere channel communication system is shown in Fig. 1. The data stream transmission is divided into an independent number of K sub-carriers, which are determined by the variations of LUF-MUF and Bandwidth coherent (B_c) values. The values of LUF-MUF and B_c are known on the transmitter and receiver sides.

The LUF and MUF values could be obtained from physics models such as the International Reference of Ionosphere (IRI) [34], the Advanced Stand-Alone Prediction System (ASAPS) [35], and NeQuick [36] that available for public uses. Those models are empirical models that were built using different methods but have a similar number of input variables, namely: location, time, and conditions of solar activity. In practice, more than one input variable could make the system more complex. Therefore, in addition to these empirical models, a method that is currently developing and has the potential to be used practically is a machine learning-based model [37]–[39]. The machine learning model could

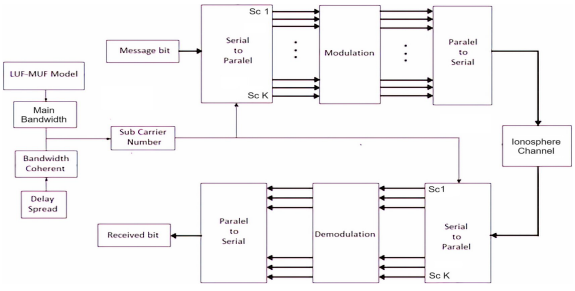

Fig. 1 Block diagram of the proposed ionosphere communication system using the multi-carrier modulation technique and LUF-MUF variations. Variations of LUF-MUF values and bandwidth coherence determine the number of sub-carriers and are known by the transmitter and receiver for optimization of available capacity usage along with reliability.

utilize a single variable of time series data. Therefore, the LUF-MUF model based on machine learning is simpler to practically apply in the proposed system. In this study, the LSTM machine learning model was used for the analysis beside the empirical physic model namely ASAPS.

The LUF-MUF values determine the main bandwidth, with a value in the range of MHz. To roughly determine the number of sub-carriers of the proposed system, the main bandwidth is divided by the Bandwidth coherent (B_c) as spacing sub-carrier frequency to avoid frequency selective fading. The B_c value is in the range of kHz and can be obtained from the delay spread value recommended by ITU [27] or from the channel sounding system as part of the channel estimation process [40], [41]. In this study, the B_c value is 2 kHz refers to the ITU delay spread value in quite ionosphere conditions, and is known by the transmitter and receiver. To calculate the total channel capacity, the equation that could be used is expressed as follows:

$$C_{tot} = \Sigma_{k=1}^{K} B_k \log_2(1 + \frac{|g_k|^2 P_k}{N_k B_k}) \tag{14}$$

where P_k is the transmit power, g_k is the channel gain, B_k is the sub-carrier bandwidth following the Bc value, and N_k is the noise spectral density values of each independent k sub-carrier. The number of K sub-carriers are determine using the following equations:

$$K_i = \frac{MUF_i - LUF_i}{B_c} \tag{15}$$

where $MUF - LUF$ is the value of the maximum-lowest usable frequency values as a function of time i, and B_c is the coherent bandwidth value. In this calculation, the maximum number of sub-carriers is assumed without using guard band frequency and the system has perfect synchronization between transmitter and receiver with no Doppler, and no time offsets.

To calculate the reliability of the proposed system, the Basic Circuit Reliability (BCR) is used according to Eq. (9). However, because the ground truth of LUF-MUF determines the success of each sub-carrier frequency transmission in the BCR calculation, the Mode Reliability (MR) calculation should be conducted first. If the sub-carrier transmission frequency is outside the actual LUF-MUF range, then the transmission of radio waves from the transmitter to the receiver cannot be realized perfectly due to some sub-carrier frequencies not being reflected by the ionosphere [3], which inherently causes the BCR values for those frequencies to be zero. To calculate the Mode Reliability of the proposed multi-carrier technique, there are two scenarios that can be used, namely:

- Scenario #1. Transmission fails completely if one or more of the sub-carriers cannot be realized, and
- Scenario #2. Transmission can still be realized with some degree of reliability, even if some sub-carriers cannot be realized.

For the Scenario #1, the Mode Reliability (MR) calculation for multi-carrier transmission could be expressed as follows:

$$\begin{aligned} MR(\%) &= \frac{1}{M}\Sigma_{m=1}^{M} P(LUF; MUF)_m .100 \\ P(LUF; MUF)_m &= \begin{cases} 1, & \text{if } LUF_{pred} \geq LUF_{act} \\ & \cap MUF_{pred} \leqslant MUF_{act} \\ 0, & \text{otherwise} \end{cases} \end{aligned} \tag{16}$$

where MR is the Mode Reliability in the M period time, LUF_{pred} and MUF_{pred} are the LUF and MUF from the model, and LUF_{act} and MUF_{act} are the actual values of LUF and MUF from observation. MR values that achieve 100% show that in periods of M, the system is reliable due to all sub-carrier transmissions being able to propagate in the ionosphere channel. However, if the MR value is less than 100%, then the system is not reliable at the period of M because one or more sub-carrier transmissions are not able to propagate in the ionosphere channel. The M period time could represent the period of an hour in one day or the period of a day in one month.

For the Scenario #2, where reliability is still realized even though there are several sub-carriers that fail to propagate in the ionosphere channel, the calculation of the Mode Reliability can be expressed by the equation:

$$\begin{aligned} MR(\%) &= \frac{\Sigma_{k=1}^{K} P(f_k)}{(\frac{MUF-LUF}{B_c})} .100 \\ P(f_k) &= \begin{cases} 1, & \text{if } LUF \leqslant f_k \leqslant MUF \\ 0, & \text{otherwise} \end{cases} \end{aligned} \tag{17}$$

where B_c is the coherent bandwidth value which determines the number of sub-carriers from the main bandwidth. LUF-MUF is the actual value from the observation, and $P(f_k)$ is the probability of each k sub-carrier frequency, which is in the range of the LUF-MUF from the model. In this scenario, even though one or more sub-carrier transmissions cannot be realized due to the ionospheric channel not supporting the propagation from the transmitter to the receiver, the system still has some degree of reliability.

4. Numerical Simulation Results

In this section we evaluate the ergodic capacity and reliability of the proposed system using numeric simulation. The simulation was done by sending a number of random message bits to each of the independent sub-carrier channels as shown in the block diagram of Fig. 1 and evaluating the achieved capacity and reliability. Parameter that used in the simulation are shown in Table 1, with assumption perfect synchronization between transmitter and receiver with no Doppler, and no time offsets which are source of Inter Symbol Interference (ISI) and Inter Carrier Interference (ICI). The sub-carrier frequencies are determined from the range of LUF-MUF values, which resulted from a model. For LUF-MUF models, we use the ASAPS and LSTM models.

Table 1 Simulation parameter values.

Parameter	Value	Description
Circuit location	Pontianak	00.01.14;S 109.20.29;E
Propagation Mode	NVIS	
Actual LUF-MUF	Ionosonde CADI	Dec2022, Jan2023
LUF-MUF Models	ASAPS and LSTM	Dec2022, Jan2023
SN_m	40-50 dB	VOACAP
SN_o	24 dB	BPSK in Rayleigh
B_c	2 kHz	Normal condition
Number of bit	10 Mbit	
Channel types	Rayleigh, AWGN	Ergodic, Upperbound

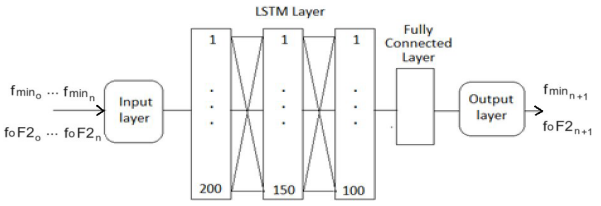

Fig. 2 Architecture of the LSTM model to predict the LUF-MUF values.

The ASAPS model is provided in the public domain and could be used openly, with its prediction performance already reported in [42]–[44]. However, for the LSTM model, we designed its architecture and tested its performance.

4.1 LSTM Model Performance

Long short-term memory (LSTM) is an artificial neural network that has a feedback connection and thus can be classified as a recurrent neural network (RNN) [45]. LSTM has been shown to outperform traditional RNNs on numerous temporal processing tasks [46]. These temporal processing tasks include the processing of multivariate time-series data to perform predictions on future values. In this research, LSTM is used to predict the LUF-MUF values with the architecture of the LSTM model presented in Fig. 2.

The model of LSTM consists of three LSTM layers and one fully connected layer, with inputs in the form of f_{min} and f_oF2 data set values. The data set was obtained from Ionosonde in Pontianak, and the period of data for the LSTM training and fitting process is December 2022. The output of the LSTM model is the prediction of the f_{min} and f_oF2 values, and its performance is evaluated based on the actual f_{min} and f_oF2 values from Ionosonde Pontianak in January 2023. The f_{min} and f_oF2 prediction values are equivalent to the LUF-MUF values for determining the main bandwidth of the proposed system. The method of the LSTM model is open-loop forecasting, where the recent observation data is reused for the future prediction process.

The prediction results of the LSTM model for the parameters f_{min} and f_oF2 as LUF-MUF equivalent values are presented in Fig. 3. Comparison of the predicted results of the LSTM model with the actual values shows that the root mean square error (RMSE) value is 0.55502 for the f_{min} parameter. As for the parameter f_oF2, the RMSE value has reached 0.56099. The RMSE value of f_{min} and f_oF2 that reaches 0.5 MHz will have a significant impact on the

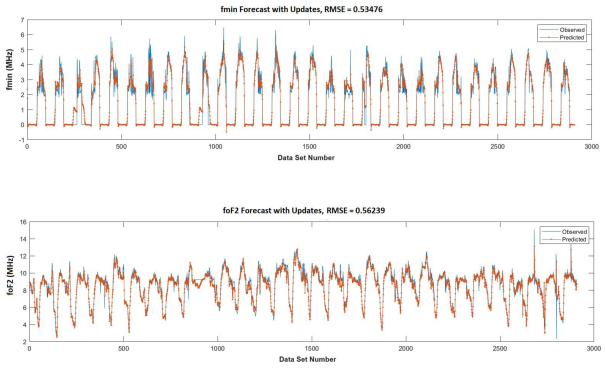

Fig. 3 Comparison between predicted values output from the LSTM model and actual values for (a) f_{min} and (b) f_oF2 in January 2023. The vertical axis is frequency, and the horizontal axis is the sequence of the predicted data set number.

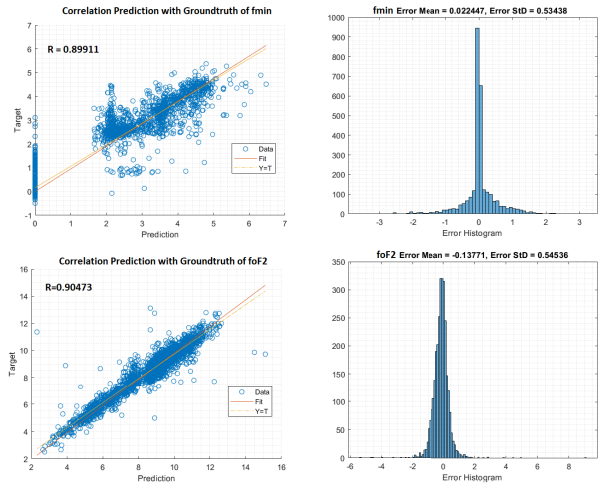

Fig. 4 Performance of LSTM model for (a) f_{min} and (b) f_oF2 prediction values.

utilization of available channels and the level of system reliability. For instance, using a 2 kHz bandwidth of subcarriers based on ITU delay spread recommendations values [27], the 0.5 MHz error prediction value lower than the actual could make around 250 subcarriers not used effectively. Meanwhile, the 0.5 MHz error prediction value higher than the actual could make around 250 subcarriers impossible to realize, which influenced the reliability of the system. Figure 4 shows the statistical analysis of the performance of the LSTM model. The correlation between the predicted results and the actual parameter f_{min} is 0.89. As for the parameter f_oF2, the correlation is 0.905. The error distribution of f_{min} has a mean 0.02247 and a standard deviation 0.53438. While the distribution of errors resulting from the prediction of f_oF2 has a mean value −0.13771 and a standard deviation of 0.54536.

4.2 Ergodic Channel Capacity

Figure 5(a) shows the results of calculating the ergodic capacity and upper limit (upper bound) of channel capacity

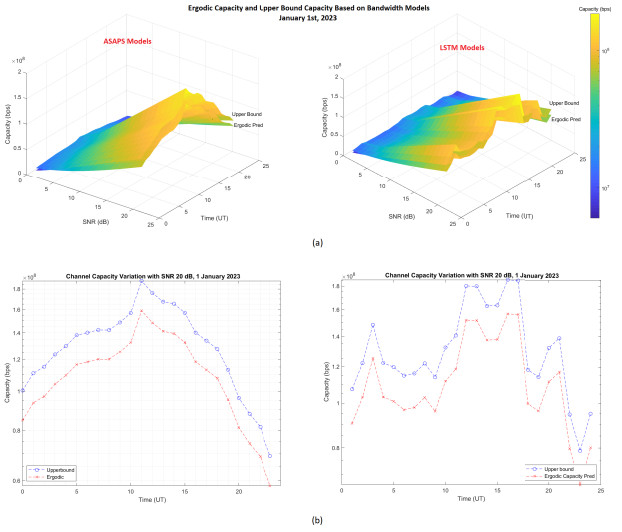

Fig. 5 Comparison of ergodic capacity using the ASAPS and LSTM models on January 1, 2023, with (a) variations of SNR 1 to 20 dB and (b) SNR 20 dB. The achieved ergodic capacity values are in the range of 10^6 to 10^8 bps, while the conventional method is below 10^3 bps [25].

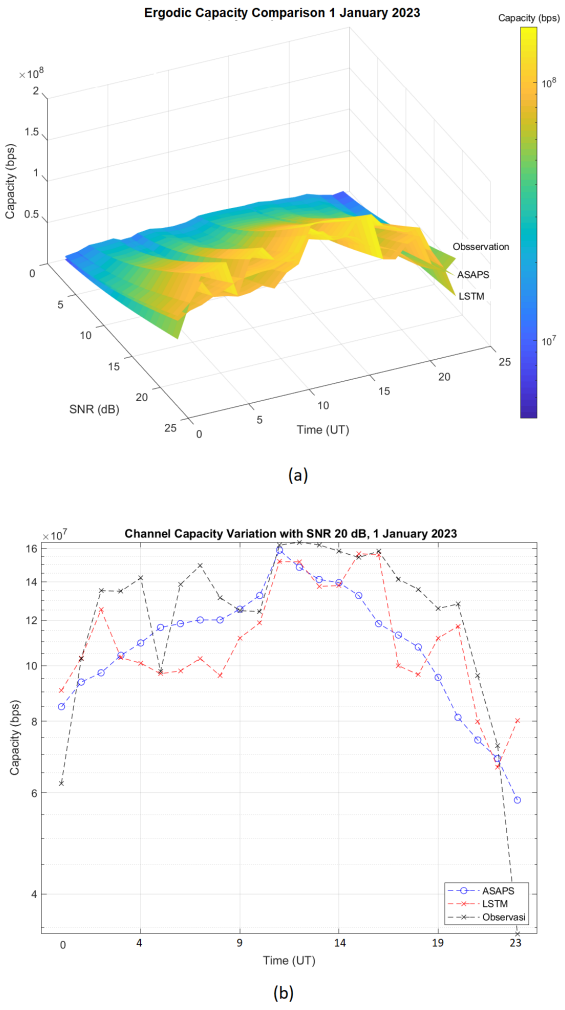

Fig. 6 Calculation of the ergodic capacity based on the main bandwidth variations from the ASAPS model, LSTM model, and actual main bandwidth on January 1, 2023, with (a) variations of SNR from 1 to 20 dB and (b) SNR 20 dB.

on January 1, 2022, based on the main bandwidth values of the LUF-MUF ASAPS and LSTM models with SNR values between 1 and 20 dB. From the figure, it can be seen that the ergodic channel capacity varies every hour, with values ranging from 10 Mbps to 100 Mbps. This achieved ergodic capacity value is higher than the existing achieved capacity, which is 9.6 kbps [25].

In Fig. 5(b), it can be seen specifically the calculation of the ergodic capacity of the channel with 20 dB SNR of two model LUF-MUF. The channel ergodic capacity using the ASAPS model shows that the minimum ergodic capacity occurs at 23 Universal Time (UT), or 6 Local Time (LT; UT+7) with a value $5.8 \cdot 10^7$ bps. Meanwhile, the maximum capacity is at 12 UT or 19 LT, with values up to $1,58 \cdot 10^8$ bps. The minimum ergodic capacity using the LSTM is $6.6 \cdot 10^8$ bps and occurs at 22 UT or 05 LT. The maximum ergodic capacity of the LSTM model occurs at 15 UT or 22 LT with values up to $1.56 \cdot 10^8$ bps.

Figure 6 depicts a comparison of ergodic channel capacity between the ASAPS model, LSTM model, and the actual values on January 1, 2023. Figure 6(a) shows the calculation of ergodic channel capacity for SNR values between 1 and 20 dB. While Fig. 6(b) shows the ergodic channel capacity with 20 dB SNR. Based on the figure, it can be seen the difference between the ergodic channel capacity value of the model and the actual value. The calculation of ergodic channel capacity using models can be higher or lower than the actual ergodic channel capacity values. This condition depends on the comparison between the LUF-MUF values of the model and the actual LUF-MUF values, which determine the main bandwidth value. When the predicted main bandwidth value from the model is lower than the actual main bandwidth (an underestimate), there is still available ergodic channel capacity that can be realized. However, when the predicted main bandwidth from the model is higher than the actual main bandwidth (an overestimate), some ergodic channel capacity cannot be realized, which affects the system's reliability.

In Fig. 6(b), the actual ergodic capacity in the 23 UT to 00 UT, or 06 LT to 07 LT, is lower than the ergodic capacity of the ASAPS and LSTM models. This condition occurs due to the lower values of the actual main bandwidth compared to the predicted main bandwidth values from the ASAPS and LSTM models. The ASAPS and LSTM models exhibited limitations in accurately predicting the lower values of actual f_{min} and f_oF2, consequently leading to higher main bandwidth and ergodic capacity when compared to the actual values. The inability of the ASAPS and LSTM models to predict the f_{min} and f_oF2 could be attributed to the "sudden change" of the f_{min} and f_oF2 trend values in those periods of time. Around 23 UT–00 UT, or 06–07 at local time, the sun begins to rise (sunrise). The formation of the ionosphere layers in this period changes from the dominant

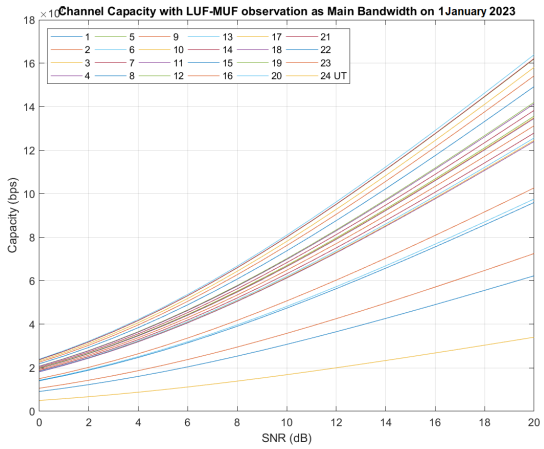

Fig. 7 Ergodic channel capacity based on the actual bandwidth value of the ionosphere channel on January 1, 2023

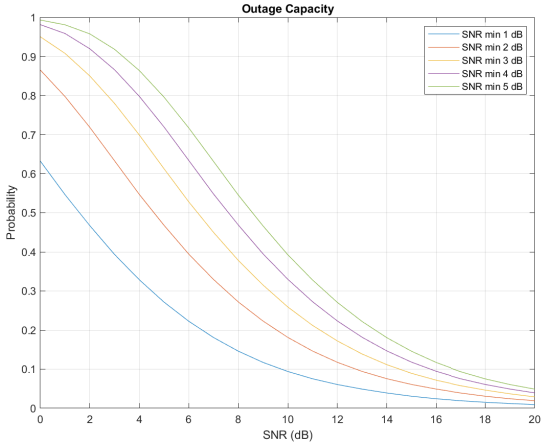

Fig. 8 Outage capacity with minimum SNR (SN_o) from 1 to 5 dB.

recombination process to the dominant ionization process as the radiation from the sun starts [47]. The trends of the f_{min} and f_oF2 values start to increase as the solar radiation increases, which is opposite to the previous trends. In addition to these conditions, the rate of the ionization process in the D layer, which determines the f_{min} values, is different from the rate of the ionization process in the F layer, which determines the f_oF2 value [48]. The f_{min} values increase faster than the f_oF2 values, which makes the actual main bandwidth lower compared to the previous values. These "sudden trend changes" could not be correctly predicted by the ASAPS and LSTM models, which resulted in a lower actual ergodic capacity value.

In Fig. 7, the calculation of ergodic channel capacity as a function of SNR for every hour on January 1, 2023, using the actual LUF-MUF value is presented. From the calculation results, it can be seen that the highest capacity occurs at 13 UT (20 LT) and the lowest capacity at 00 UT (07 LT). When the SNR is 0 dB, the difference in capacity between the minimum and maximum is 10 Mbps. Meanwhile, at 20 dB SNR, the difference reaches 100 Mbps.

In Fig. 8, the outage capacity with a minimum SNR value between 1 and 5 dB is presented as a general calculation of the reliability level of communication systems in the Rayleigh distributed channel. It can be seen that an increase in the SNR minimum or threshold value is followed by an increase in the outage capacity. If the SNR value on the receiving side increases and the minimum SNR value remains constant, the outage capacity value decreases.

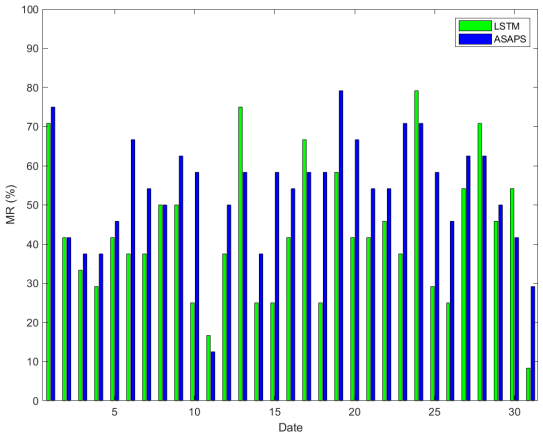

Fig. 9 Mode reliability calculation result for each day in January 2023 using Scenario #1.

4.3 Reliability

Figure 9 shows the calculation of the Mode Reliability for each day in January 2023 with the first scenario based on Eq. (16). The M period of this Mode Reliability calculation is for each day in one month. From Fig. 9, it can be seen that the Mode Reliability using the LUF-MUF value from the ASAPS model in January 2023 is in the range of 10% to 79%, and the Mode Reliability using the LSTM model is in the range of 8% to 79%. The lowest value of Mode Reliability in the ASAPS model is 10%, which occurs on January 11, while the highest value of Mode Reliability is 79% and occurs on January 19. The lowest value of Mode Reliability of the LSTM model is 8% and occurs on January 31, while the highest value of Mode Reliability is 79% and occurs on January 24, 2023.

To get a more detailed explanation of calculation results from Mode Reliability values using Scenario #1, which is given in Fig. 9, a good example of comparative data between the LUF-MUF model values and the actual LUF-MUF values from observation over one day, namely January 6, 2023, is presented in Fig. 10. It can be seen that on January 6, 2023, between 11 and 22 UT, the LUF and MUF values of the ASAPS model are between the actual LUF-MUF values. This condition is considered reliable because the range of subcarrier frequencies that were selected in the transmission system could be realized. Different conditions occurred between 6 UT and 11 UT. The LUF-MUF value of the ASAPS model is outside the range of the actual LUF-MUF values, where the LUF model is lower than the actual LUF. Therefore, the system is considered unreliable because all the selected sub-

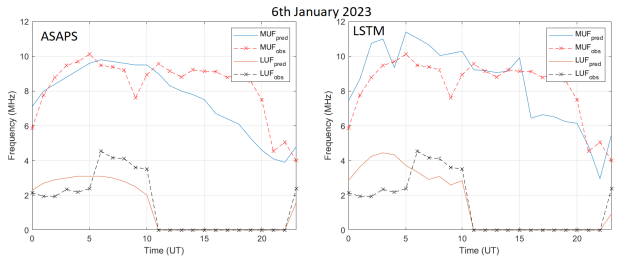

Fig. 10 Comparison of actual LUF-MUF values with results from (a) ASAPS, and (b) LSTM models on 6th January 2023.

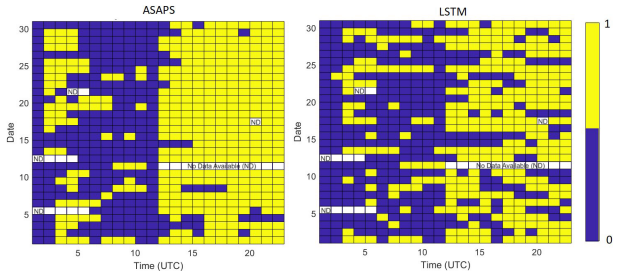

Fig. 11 Mode reliability for each hour in January 2023 using Scenario #1. The yellow box color indicates the system is reliable. While the blue box color indicates the unreliability of the system, The white color with 'No Available Data (ND)' marks shows the unavailable MR calculation results due to the unavailable data of the actual LUF-MUF.

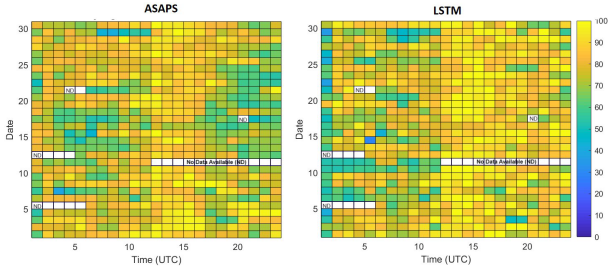

Fig. 12 Mode Reliability for each hour in January 2023 using Scenario #2. The MR values are presented in color. The white color with 'No Available Data (ND)' marks shows the unavailable MR calculation results due to the unavailable data of the actual LUF-MUF.

carrier frequencies could not be fully realized. At different time periods, namely 0 UT to 1 UT, it can be seen that the predicted LUF value of the ASAPS model is within the range of actual LUF-MUF values. However, the predicted MUF value is outside the range of actual LUF-MUF values, which is considered to be an unreliable system. This condition explains why the ASAPS Mode Reliability value reached 68% on January 6, 2022, as shown in Fig. 9. Similar to the ASAPS model, some of the predicted LUF and MUF values from the LSTM models are within the range of the actual LUF-MUF values, which occurred between 16 and 22 UT, and are considered reliable. Meanwhile, the predicted LUF and MUF values between 6 UT and 10 UT were outside the range of the actual LUF-MUF values, which caused the system to be considered unreliable.

In Fig. 11, the Mode Reliability calculation result using the first scenario for every hour of every day in January 2023 based on Eq. (16) is presented. The M period of this Mode Reliability calculation is for each hour in one day. The blue color represents a system considered unreliable, while the yellow color represents a system considered reliable. In every hour of the day, if the LUF-MUF from the model is within the range of the actual LUF-MUF, the system is considered reliable at that hour. However, if some values of the LUF-MUF from the model were outside the actual LUF-MUF, the system is considered not reliable at that hour due to the fact that one or more of the sub-carriers could not be realized. From the figure, it can be seen that the dominant reliable system occurs from 17 UT to 23 UT, which is at night in local time. The dominance of a reliable system at night can be attributed to the very low f_{min} value parameter due to the disappearance of the D layer during nighttime [49]. With the disappearance of the D ionosphere layer, the determination of the main bandwidth only depends on the accuracy of the MUF value prediction.

Figure 12 is the second scenario Mode Reliability calculation result, which shows the hourly variations of MR values on each day in January 2023 for the ASAPS and LSTM models. For each hour in a day, there are no zero values for MR, which indicates the total failure of transmission. However, there are a number of hours for which the MR value cannot be calculated due to the unavailability of the actual LUF-MUF, which are on the 5th, 11th, 12th, 17th, and 21st. The unavailable MR calculation values are shown in a white color box with the 'No Available Data (ND)' mark. Based on the calculations, the Mode Reliability of the LSTM model shows a high value for each day from 12 UT to 20 UT, which reaches up to 100%. As for the ASAPS model, the highest value of Mode Reliability is in the range of 13 UT to 16 UT. The 100% value of Mode Reliability indicates that all sub-carrier transmissions based on the range of LUF and MUF model values are acceptable because the ionosphere layer is able to support the propagation. The Mode Reliability value that is less than 100% indicates that a number of sub-carrier transmissions fail due to being outside the range of the actual MUF-LUF value. Fluctuations in the Mode Reliability level indicate that transmission from each sub-carrier for every hour of the day cannot be fully realized. There are several sub-carrier transmissions experiencing problems as the LUF and MUF model values do not match the actual LUF and MUF values. The lowest value of the second scenario Mode Reliability calculation for both ASAPS and LSTM models is in the range of 40%.

The calculation of Mode Reliability in Fig. 12 shows the reliability fluctuations of the selected sub-carriers based on the realization of available sub-carriers. For each sub-carrier frequency that can be used, the BCR value can be calculated using equation (9) with monthly SNR (SN_m) values based on the VOACAP prediction model (Fig. 13(a)), SN_o values based on the BER versus SNR curve using BPSK modulation (Fig. 13(b)) for BER values of 10^{-3}, and D_l values based on the ITU table (ITU, 1999). Using Eq. (9), the BCR value for a single sub-carrier frequency

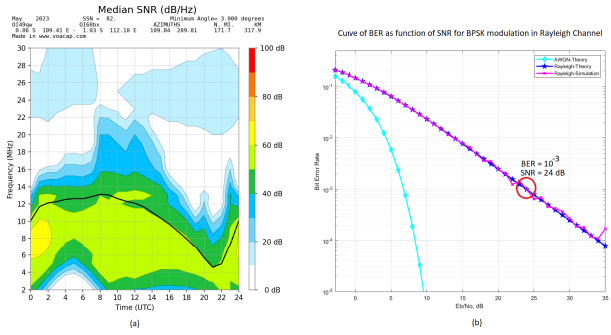

Fig. 13 (a) Monthly SNR prediction from the VOACAP model, and (b) BER versus SNR curve for BPSK modulation in Rayleigh distributed channel. The SN_o values can be determined based on acceptable BER values.

is $130 - 80/[1 + (50 - 24)/8].1.1 = 111.1765\%$ or 100%. Because the SN_m value presented in Fig. 13(a) is quite uniform over the range of LUF-MUF values, this value can also be used as a representation of the BCR value for all sub-carrier frequencies, which is 100%. This result also affects the calculation of the BRR value using Eq. (13) with a 100% reliability. Even though the BRR value is 100%, it should be noted that this value is limited by the selection of the sub-carrier frequency in the range of the actual LUF-MUF value only. The LUF-MUF values from the model can be different from the actual LUF-MUF values. Therefore, the optimization of channel capacity and reliability in this system is determined by the accuracy factor of the LUF-MUF value model, whose function is the determination of the main bandwidth value.

5. Conclusion

The multi-carrier modulation technique, combined with LUF-MUF variation, is a promising method for improving the channel capacity while also maintaining the reliability of the ionospheric communication channel system. This method uses variations of LUF-MUF prediction values from a model as the main bandwidth and a Bandwidth coherent B_c value as the subcarrier bandwidth. Numeric simulation using the ASAPS and LSTM models for the LUF-MUF values shows the achieved ergodic channel capacity varies in a range of 10 Mbps to 100 Mbps with SNR 0 to 20 dB. While the reliability level of the system using two scenarios of Mode Reliability calculation shows the values are in the range of 8% and 100% for every hour of the day. The simulation was conducted in Near Vertical Incidence Skywave (NVIS) propagation mode over the Pontianak region in January 2023 with the assumption of perfect synchronization, no Doppler, and no time offsets. The result also shows that the optimization of capacity and reliability were determined by the accuracy level of LUF-MUF models. If the model predicts lower LUF-MUF range values than the actual, the reliability level is maximized, but several of the available subcarrier bandwidths are not utilized. However, if the model predicts a higher LUF-MUF range value than the actual, the utilization of all the available subcarrier bandwidth is maximized, but sacrificing the reliability level to be low due to some of the sub-carrier transmissions cannot be realized.

Acknowledgments

We would like to express our sincere gratitude to our supervisor, Professor Adit Kurniawan, for his valuable guidance and support throughout the research process. This work was supported by the Research Organization for Aeronautics and Space in DIPA 2023 for Space Research Center.

References

[1] K. Davies, Ionospheric radio propagation, US Department of Commerce, National Bureau of Standards, 1965.
[2] S. Salous and L. Khadra, "Measuring the coherence of wideband dispersive channels," Electron. Commun. Eng. J., vol.1, no.5, pp.205–209, 1989.
[3] N.M. Maslin, HF Communications: A Systems Approach, CRC Press, 2017.
[4] J.E. Nilsson and T.C. Giles, "Wideband multi-carrier transmission for military HF communication," MILCOM 97 Proceedings, IEEE, 1997.
[5] H. Zhang, H. Yang, R. Luo, and S. Xu, "Design considerations of a new HF modem and performance analysis," 2005 IEEE International Symposium on Microwave, Antenna, Propagation and EMC Technologies for Wireless Communications, pp.760–763, IEEE, 2005.
[6] J.W. Nieto, "An investigation of coded OFDM and OFDM-CDMA waveforms utilizing different modulation schemes on HF multipath/fading channels," Proc. 2005 European Conference on Circuit Theory and Design, 2005, pp.III-65–68, IEEE, 2005.
[7] H. Chen and C. Jian, "Application research of technology combining AMC and OFDM in HF communication systems," 2010 6th International Conference on Wireless Communications Networking and Mobile Computing (WiCOM), pp.1–6, IEEE, 2010.
[8] J.L. Pijoan, D. Altadill, J.M. Torta, R.M. Alsina-Pagès, S. Marsal, and D. Badia, "Remote geophysical observatory in antarctica with HF data transmission: A review," Remote Sensing, vol.6, no.8, pp.7233–7259, 2014.
[9] G. Earl and B. Ward, "The frequency management system of the jindalee over-the-horizon backscatter HF radar," Radio Science, vol.22, no.2, pp.275–291, 1987.
[10] J.M. Goodman, Space Weather & Telecommunications, Springer New York, NY, 2005.
[11] J. Wang, Y. Shi, C. Yang, and F. Feng, "A review and prospects of operational frequency selecting techniques for HF radio communication," Advances in Space Research, vol.69, no.8, pp.2989–2999, 2022.
[12] R. Adair, "An automatic link establishment standard for automated digital HF radios," IEEE Military Communications Conference,'Bridging the Gap. Interoperability, Survivability, Security', pp.853–864, IEEE, 1989.
[13] W. Furman and E. Koski, "Next generation ALE concepts," IET 11th International Conference on Ionospheric Radio Systems and Techniques (IRST 2009), pp.152–156, 2009.
[14] A. Haghbin, M. Khodaverdizadeh, and F. Razzazi, "Improving the performance of hf radio networks in presence of interference: Frequency hopping automatic link establishment," 2022.
[15] Z. Zhang, F. Zeng, L. Ge, S. Chen, B. Yang, and G. Xuan, "Design and implementation of novel hf ofdm communication systems," 2012 IEEE 14th International Conference on Communication Technology, pp.1088–1092, IEEE, 2012.
[16] A. Ismail and K. Mohamedpour, "Performance study of HF communication using NOMA over narrowband HF channel," 2022.
[17] J. Nieto, "Constant envelope waveforms for use on HF multipath

fading channels," MILCOM 2008 — 2008 IEEE Military Communications Conference, pp.1–5, IEEE, 2008.
[18] M.F.G. Garcia, J.M. Paez-Borrallo, and S. Zazo, "Efficient pilot patterns for channel estimation in OFDM systems over HF channels," Gateway to 21st Century Communications Village. VTC 1999-Fall. IEEE VTS 50th Vehicular Technology Conference (Cat. no.99CH36324), pp.2193–2197, IEEE, 1999.
[19] P. Bechet, S. Miclaus, A. Miclaus, and C. Balint, "Experimental analysis of noise level and channels availability for high frequency OFDM data transmission in NVIS propagation conditions," 2016 International Symposium on Electromagnetic Compatibility-EMC EUROPE, pp.844–849, IEEE, 2016.
[20] C. Lamy-Bergot, A. Kermorgant, F. Gourgue, J.Y. Bernier, H. Diakhaté, and J.L. Rogier, "Wideband HF transmissions: Operating in a crowded spectrum," THALES Communications & Security, vol.92622, p.10, 2016.
[21] A.A. Ibrahim, A. Abdelaziz, and M.M. Salah, "On the performance of OFDM and single carrier communication over wideband HF channel: Theory and practice," Telecommun. Syst., vol.77, no.4, pp.671–682, 2021.
[22] A.A. Ibrahim, A.M. Abdelaziz, and M.M. Salah, "OFDM over wideband ionospheric HF channel: Channel modelling & optimal subcarrier power allocation," 2018 35th National Radio Science Conference (NRSC), pp.300–308, IEEE, 2018.
[23] Z. Qin, J. Wang, J. Chen, G. Ding, Y.D. Yao, X. Ji, and X. Chen, "Link quality analysis based channel selection in high-frequency asynchronous automatic link establishment: A matrix completion approach," IEEE Syst. J., vol.12, no.2, pp.1957–1968, 2017.
[24] R. Desourdis and E. Johnson, "Advanced link quality analysis for ALE HF radio," Proc. MILCOM'93-IEEE Military Communications Conference, pp.91–95, IEEE, 1993.
[25] W.N. Furman and J. Nieto, "Latest on-air testing of U.S. mil-std-188-110c appendix D wideband HF data waveforms," 12th IET International Conference on Ionospheric Radio Systems and Techniques (IRST 2012), 2012.
[26] C. Mudzingwa and A. Chawanda, "Radio propagation prediction for HF communications," Communications, vol.6, no.1, pp.5–12, 2018.
[27] ITU, "ITU-R REC. F.1487: Testing of HF modems with bandwidths of up to about 12 kHz using ionospheric channel simulators," International Telecommunication Union, Radiocommunication Sector, Geneva, 2000.
[28] L.F. McNamara, The Ionosphere: Communications, Surveillance, and Direction Finding, Krieger Publishing Company, 1991.
[29] M.C. Walden, "High-frequency near vertical incidence skywave propagation: Findings associated with the 5 MHz experiment," IEEE Antennas Propag. Mag., vol.58, no.6, pp.16–28, 2016.
[30] B.A. Witvliet and R.M. Alsina-Pagès, "Radio communication via near vertical incidence skywave propagation: An overview," Telecommun. Syst., vol.66, pp.295–309, 2017.
[31] I.T.U.R.S. (ITU-R), "Computation of reliability and compatibility of HF radio systems," 2007.
[32] A. Stocker, "Fast and accurate calculation of multipath spread from VOACAP predictions," Radio Science, vol.47, no.4, pp.1–10, 2012.
[33] A. Goldsmith, Wireless Communications, Cambridge University Press, 2005.
[34] D. Bilitza, "IRI the international standard for the ionosphere," Adv. Radio Sci., vol.16, pp.1–11, 2018.
[35] L.F. McNamara, C.R. Baker, and W.S. Borer, "Real-time specification of HF propagation support based on a global assimilative model of the ionosphere," Radio Science, vol.44, no.1, pp.1–13, 2009.
[36] S.M. Radicella and B. Nava, "Nequick model: Origin and evolution," Proc. 9th International Symposium on Antennas, Propagation and EM Theory, pp.422–425, IEEE, 2010.
[37] J. Wang, C. Yang, and W. An, "Regional refined long-term predictions method of usable frequency for HF communication based on machine learning over asia," IEEE Trans. Antennas Propag., vol.70, no.6, pp.4040–4055, 2021.
[38] M.A. Ameen, A. Tahir, M. Talha, H. Khursheed, I.A. Siddiqui, S.T. Iqbal, and B. Gul, "Modelling of $f_o F_2$ using artificial neural network over equatorial ionization anomaly (EIA) region stations," Advances in Space Research, vol.72, no.12, pp.5539–5550, 2023.
[39] R. Atıcı and Z. Pala, "Prediction of the ionospheric $f_o F_2$ parameter using R language forecasthybrid model library convenient time series functions," Wireless Pers. Commun., vol.122, no.4, pp.3293–3312, 2022.
[40] X. Tuo, W. Cheng, R. Yang, and H. Cheng, "The performance comparison of the channel estimation methods base on pilots symbol interpolation in HF OFDM system," 2015 3rd International Conference on Mechatronics and Industrial Informatics (ICMII 2015), pp.563–570, Atlantis Press, 2015.
[41] R.C. Cannizzaro, P. Banelli, and G. Leus, "Adaptive channel estimation for OFDM systems with Doppler spread," 2006 IEEE 7th Workshop on Signal Processing Advances in Wireless Communications, pp.1–5, IEEE, 2006.
[42] C. Brousseau, V. Gasse, and L. Bertel, "Comparison of three HF ionospheric prediction models (ASAPS, VOACAP, LOCAPI)," 8th International Ionospheric Effect Symposium, 1996.
[43] R. Barnes, R. Gardiner-Garden, and T. Harris, "Real time ionospheric models for the australian defence force," Proc. WARS-2000, vol.122135, pp.122–135, 2000.
[44] R. Malik, M. Abdullah, S. Abdullah, M.J. Homam, T. Yokoyama, and C. Yatini, "Prediction and measurement of high frequency radio frequencies in peninsular malaysia and comparisons with the international reference ionosphere model," Advanced Science Letters, vol.23, no.2, pp.1294–1298, 2017.
[45] S. Hochreiter and J. Schmidhuber, "Long short-term memory," Neural Computation, vol.9, no.8, pp.1735–1780, 1997.
[46] F.A. Gers, D. Eck, and J. Schmidhuber, "Applying LSTM to time series predictable through time-window approaches," International Conference on Artificial Neural Networks, pp.669–676, Springer, 2001.
[47] T. Yonezawa, "Theory of formation of the ionosphere," Space Sci. Rev., vol.5, no.1, pp.3–56, 1966.
[48] W. Webber, "The production of free electrons in the ionospheric *D* layer by solar and galactic cosmic rays and the resultant absorption of radio waves," J. Geophysical Research, vol.67, no.13, pp.5091–5106, 1962.
[49] F. Gardner and J. Pawsey, "Study of the ionospheric D-region using partial reflections," Journal of Atmospheric and Terrestrial Physics, vol.3, no.6, pp.321–344, 1953.

Varuliantor Dear received the M.S. degrees in Electrical Engineering from Bandung Institute of Technology in 2015. Currently, he is a Doctor candidate in Bandung Institute of Technology and also works in the Space Research Center, National Institute and Innovation Agency Indonesia with research scope is the ionospheric channel propagation

Annis Siradj Mardiani received the B.S. degrees in Electrical Engineering from Achmad Yani University Indonesia, she works in the Space Research Center, National Institute and Innovation Agency Indonesia with research scope is the space weather impact to the ionosphere.

Nandang Dedi works at Space Research Center, National Institute and Innovation Agency Indonesia as a research assistant. His research scope is in Ionosphere Space weather information services.

Prayitno Abadi received his Doctorate degree from Nagoya University. Currently, he is a senior researcher at the Research Center for Climate and Atmosphere in the National Research and Innovation Agency of Indonesia, with research interests focusing on ionospheric effects on radio wave propagation. Additionally, he also serves as a lecturer for digital signal processing at Telkom University, Indonesia.

Baud Haryo Prananto received a B.S. degree from Bandung Institute and Technology, Indonesia in 2004 and M.S. degree from Korea Institute of Science and Technology, South Korea in 2008. Currently, he is studying at Bandung Institute of Technology as a Doctoral student. He is currently working as a Specialist Trainer in Nokia Solutions and Networks since 2008, delivering training related to 4G and 5G RAN Nokia equipment.

Iskandar received the M.S. and PhD degrees in Electrical Engineering from Bandung Institute of Technology and Waseda University, respectively. Currently, He is a lecture in Bandung institute of Technology.